Theoretical results on the latitude dependence of the Kelvin-Helmholtz instability at the dayside magnetopause for northward interplanetary magnetic fields

Julia E. Contin[1]
Universidad Tecnológica Nacional, Regional Haedo, Pcia. Buenos Aires, Argentina

Fausto T. Gratton
Instituto de Física del Plasma, FCEyN-Universidad de Buenos Aires/CONICET, Argentina

Charles J. Farrugia
Space Science Center, University of New Hampshire, Durham, New Hampshire, USA

Received 8 February 2002; revised 17 October 2002; accepted 12 December 2002; published 4 June 2003.

[1] We study the Kelvin-Helmholtz (KH) instability at the dayside magnetopause, modeling the flow, the magnetic field, and the density profiles in the transition from magnetosheath to magnetosphere with hyperbolic tangent functions. The strength and the direction of the fields on the sunward sides of the magnetopause are obtained from a MHD simulation code of the magnetosheath, which includes the magnetic tension forces on the plasma in the plasma depletion layer. The theory is applied to strongly northward interplanetary magnetic fields. We work at slightly off-noon local times and compute at three different latitudes. We find that as the latitude increases the instability growth rate becomes negligible due to the increasing local magnetic shear, which reaches $\sim 21^\circ$ at the highest latitude examined. The KH growth rates for the most unstable modes are given as functions of λ/Δ, the ratio of the wavelength to the width of the transition. The KH perturbation tends to be localized on the magnetospheric side when the configuration is most unstable, whereas it shifts increasingly toward the magnetosheath side of the velocity gradient region as the latitude increases and the growth rate diminishes substantially. Growth rates for a tangential discontinuity model are within a 10% of those corresponding to continuous profiles when $\lambda > 15\Delta$. The influence of temporary (sunward or earthward) accelerations of the magnetopause on the KH modes is examined. The effect of a difference between the scale length of the density profile and the width of the current sheath on the KH instability, as in pristine magnetopauses, is also studied. *INDEX TERMS:* 2724 Magnetospheric Physics: Magnetopause, cusp, and boundary layers; 2752 Magnetospheric Physics: MHD waves and instabilities; 2753 Magnetospheric Physics: Numerical modeling; 7871 Space Plasma Physics: Waves and instabilities; *KEYWORDS:* Dayside magnetopause, magnetopause instabilities, Kelvin-Helmholtz instability, solar wind - magnetosphere interaction, Rayleigh-Taylor instability

Citation: Contin, J. E., F. T. Gratton, and C. J. Farrugia, Theoretical results on the latitude dependence of the Kelvin-Helmholtz instability at the dayside magnetopause for northward interplanetary magnetic fields, *J. Geophys. Res.*, *108*(A6), 1227, doi:10.1029/2002JA009319, 2003.

1. Introduction

[2] Very early in the development of space physics, the Kelvin-Helmholtz (KH) instability at the magnetopause was suggested as a means for enhancing the transfer of solar wind momentum to the magnetosphere [*Dungey*, 1954]. The presence of surface waves of KH origin on the magnetopause is also interesting because they are thought to be one major source of ULF fluctuations of the geomagnetic field in the Pc 5 range (1–10 mHz) via a complex coupling with magnetospheric modes and resonant shells (e.g., *Kivelson and Southwood* [1986], and references therein).

[3] Compared to other mechanisms such as reconnection, however, the importance of the KH instability is still today a matter of study and debate. Nevertheless, the anomalous viscous drag that KH generates [*Miura*, 1984] has attracted plenty of interest particularly when northward interplanetary magnetic field (IMF) conditions prevail, because reconnection processes, that are also sources of momentum transfer, are then less likely to occur. Summaries of the main experimental, theoretical, and computational achievements

[1] Also research associate at Instituto de Física del Plasma, FCEyN-UBA/CONICET, Buenos Aires, Argentina.

0148-0227/03/2002JA009319

in this field, and the status of several open questions, can be found in many surveys such as those of *Belmont and Chanteur* [1989], *Kivelson and Chen* [1995], *Miura* [1995a], *Farrugia et al.* [1998a, 2001].

[4] This paper presents a theoretical study of the KH instability at the dayside magnetopause for northward IMF conditions, where we compute the stability of models with continuous profiles for the magnetic field and the velocity field (represented by hyperbolic tangent functions) at different latitudes on the magnetopause, to examine the stabilizing effect of the local magnetic shear angle. Even when the IMF points due north, the local shear increases with latitude because of the draping of magnetosheath magnetic field lines over the magnetopause. At the same time, the magnetosheath velocity also increases with latitude which, in turn, might counteract the effect of shear.

[5] Some aspects that we have taken into account in this work are the following. From a statistical study of low-latitude, multiple crossings of the magnetopause made by ISEE 1 and 2 over a 10-year period, *Song et al.* [1988] concluded that for northward IMF the solar wind dynamic pressure may be sufficient to explain magnetopause surface oscillations with periods in the 2–30 min range, and so KH would be at most a secondary effect. However, a detailed study by *Ogilvie and Fitzenreiter* [1989], based on ISEE 1 high resolution data, favored the generation of magnetopause surface waves by KH, with the qualification that it is necessary to distinguish the instability of the magnetopause boundary from that of the inner edge of the boundary layer (IEBL). In principle, both boundaries could go unstable, but the *Ogilvie and Fitzenreiter* [1989] results indicate that the IEBL should be more prone to the instability, while the magnetopause should be much less oscillatory. Related to this question, one of the aims of the present work is to examine on which side of the velocity gradient region is the amplitude of the KH modes larger. Later work on large-amplitude, long-wavelength magnetopause oscillations on the near-equatorial magnetopause flank under northward IMF conditions has provided new experimental evidence in support of the presence of KH activity on this boundary (e.g., *Chen and Kivelson* [1993], *Chen et al.* [1993]). In the analyses of *Chen and Kivelson* [1993] and *Chen et al.* [1993], solar wind dynamic pressure changes could be excluded as the cause of the oscillations from records of solar wind data during the events. The study of multiple magnetopause crossings on the near flanks by *Seon et al.* [1995], is also indicative of the presence of surface waves propagating tailwards, with the KH instability as a probable cause. Furthermore, *Farrugia et al.* [2000] used Interball/tail data to study the state of the near-tail magnetopause during the passage of a high density filament early on January 11, 1997 [*Burlaga et al.*, 1998]. This boundary was very oscillatory due to large amplitude waves, possibly originated from active regions on the front side and propagating toward the flanks.

[6] Another aspect of the magnetopause physics associated with the influence of the magnetosheath magnetic field orientation on the KH instability has been investigated by *Miura* [1995b] with numerical simulations carried out for Alfvénic Mach number ≥ 1 and plasma beta ≥ 1.2 (magnetosheath values). *Miura* [1995b] found that northward IMFs are more favorable to the instability than those pointing southward, and that the magnetopause oscillates most strongly when the magnetosheath magnetic field is due north.

[7] In a study of the stability of the magnetopause frontside related to the present paper, theoretical charts of the KH activity on the dayside were presented for the first time by *Farrugia et al.* [1998b]. This work, which was specifically elaborated for northward IMF configurations, was computed with a model that takes into account the all-important presence of the plasma depletion layer (PDL). The PDL is a thin layer that is generally present next to the sunward side of the magnetopause when the IMF points north [*Phan et al.*, 1994]. In the PDL the influence of magnetic forces on the plasma flowing past the magnetosphere is strong, altering the flow topology from stagnation point to stagnation line flow [*Sonnerup*, 1974]. The modification of the flow and magnetic fields in the PDL has a direct bearing on the KH instability. The influence of the IMF clock angle θ (i.e., the angle between the IMF and the geomagnetic north) on the position, shape, and size of the KH active regions is emphasized in *Farrugia et al.* [1998b]. On the dayside magnetopause, the KH instability is ordinarily tightly regulated by θ. It was shown in the same reference that even when θ is zero at the subsolar point (due north IMF) the local magnetic shear angle is not zero at other positions on the magnetopause, as a consequence of the three dimensional field draping over the frontside.

[8] In the present paper we carry out an extension of that work. The stability analysis was based on profiles having two tangential discontinuities corresponding to the magnetopause and the IEBL, respectively. By contrast, here we examine continuous profiles. The KH eigenvalue problem with velocity gradient profiles for the magnetopause was studied, e.g., by *Miura and Pritchett* [1982], and *Miura* [1995b]. Our main purpose is to investigate the properties of the KH excitation as a function of latitude, incorporating variations of the background fields across a boundary of finite thickness. The velocity and the magnetic fields change direction and intensity with position on the magnetopause, and we take into account the variations at different locales by using values for the field and flow given by results of a magnetosheath MHD simulation model [*Erkaev*, 1988; *Farrugia et al.*, 1998b].

[9] Figure 1 shows an example of the results of this model. The distribution of the magnetic shear angle is indicated, the white regions corresponding to zero magnetic shear, while the darker shading represents regions with 40 degrees or more. We can see how the magnetic shear angle increases with the latitude. The velocity field is depicted by the small arrows: the trend of the flow to align itself orthogonal to the IMF (here set at zero clock angle) is apparent, so that the flow is not symmetric about the subsolar point, and rather looks as a stagnation line flow. The effect is due to magnetic tension forces on the plasma close to the magnetopause, which are properly incorporated in the MHD code. This feature is in agreement with observational studies of properties of the plasma depletion layer for low magnetic shear [*Phan et al.*, 1994].

[10] At any given position we use a parallel velocity flow across the boundary, in agreement with the viscous magnetosphere concept, where the flow in the magnetopause is

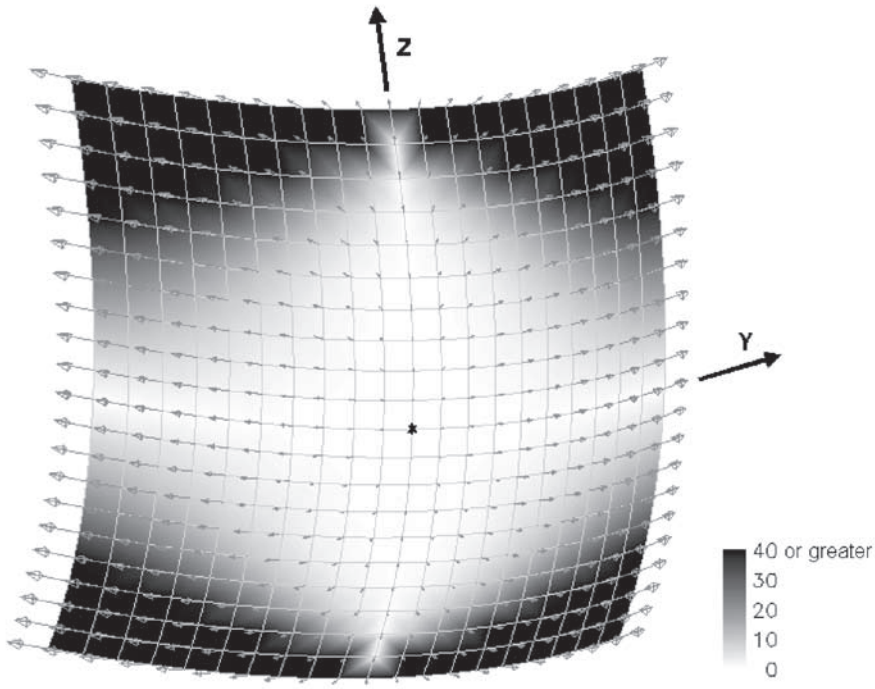

Figure 1. Spatial distribution of the magnetic shear angle, in gray scale, and the velocity field, represented by arrows, over the dayside magnetopause for an IMF with zero clock angle, as predicted by an MHD code for the magnetosheath (see text).

induced from the magnetosheath by viscous drag (about the so-called ''viscous paradigm'' see, e.g., *Kennel* [1995]). Hence, the velocity field is assumed to retain the same direction as in the adjacent magnetosheath and to approach zero in the magnetosphere. In the three magnetopause positions that we analyze, we study the variation of the maximum growth rate with the wavelength-to-width ratio, and the shape of the corresponding eigenfunctions, to examine which part of the gradient region is more perturbed: the magnetosheath or the magnetosphere side (and hence to infer which of the two regions is more wavy).

[11] The MHD equations for the KH perturbations are treated in the incompressible approximation, since the magnetosheath velocity on the frontside is much smaller than the local speed of sound, C_s. When compressibility is retained, a set of perturbation modes, the main branch (with the largest growth rate) tends to the incompressible KH modes as $C_s \rightarrow \infty$. But there is also another set of modes (with much smaller growth rates) that depend critically on compressibility, and disappear in the limit $C_s \rightarrow \infty$. The paper does not study the influence of compressibility on the KH instability, a subject that deserves further investigations [see, e.g., *Miura and Pritchett*, 1982; *Kivelson and Pu*, 1984; *González and Gratton*, 1994]. For the study of the KH modes with the largest growth rates, in subsonic regions of the dayside magnetopause, the incompressible approximation is sufficient [*González et al.*, 2002]. The influence of compressibility, however, is very important for the analysis of the KH excitation at the supersonic flanks of the magnetopause.

[12] In addition, we study the enhancement of the KH instability due to sunward accelerations of the frontside magnetopause, as well as the reduction of the excitation by earthward accelerations, by the Rayleigh-Taylor effect, as may happen during sudden changes in the solar wind dynamic pressure [*Mishin*, 1993; *Gratton et al.*, 1996]. Finally, we also examine the influence of a difference between the thickness of the density transition and the thickness of the current layer, on the KH instability. The possibility of the presence of two different length scales in magnetopauses called ''pristine'', i.e., those observed without the adjoining magnetospheric boundary layer, is discussed in a statistical study of magnetopause crossings by *Eastman et al.* [1996].

[13] Summarizing, the paper is directly related to some of the questions raised by *Farrugia et al.* [1998b, 2000]: (1) the effect of continuous profiles on the dayside KH instability; (2) the latitude dependence; (3) the effect of temporary accelerations; and (4) the effect of a scale length in the density gradient different from the thickness of the current layer and the velocity gradient region. The layout of the paper is as follows. The model of the magnetopause transition and the KH perturbative theory is explained in section 2. In section 3 we give the main results of the stability analysis, while in section 4 we consider the stability of a double-scale length magnetopause. The last section contains our conclusions.

2. Magnetopause Model and Perturbative Equations

[14] At a given position on the magnetopause, the equilibrium magnetic field $\mathbf{B_0}$ and flow velocity $\mathbf{v_0}$ across the

magnetopause and parallel to its tangent plane are given by equations of the form

$$\mathbf{v_0}(y) = v_{0x}(y)\hat{\mathbf{x}} + v_{0z}(y)\hat{\mathbf{z}},$$

$$\mathbf{B_0}(y) = B_{0x}(y)\hat{\mathbf{x}} + B_{0z}(y)\hat{\mathbf{z}}.$$

Here $\hat{\mathbf{x}}$, $\hat{\mathbf{z}}$, are unit vectors in the local tangent plane, and y is along the outward-pointing normal to the magnetopause. Equilibrium quantities are denoted by a zero subscript. The y-dependence of the fields accounts for possible changes in direction and intensity across the magnetopause, in particular, the presence of shear of the magnetic lines. Passing from the magnetosheath to the magnetosphere $\rho_0 = \rho_0(y)$ indicates the change of density. A gravity term, of the form $\mathbf{g} = -g\hat{\mathbf{y}}$, is also assumed to act along the y axis, where g is equivalent to the local acceleration of the magnetopause, as may occur when the solar wind dynamic pressure varies, $g > 0$ corresponding to a sunward acceleration. Normally we set $g = 0$, except when studying episodes of transient acceleration.

[15] G. I. Taylor noted that the theory of instability of an interface between two fluids that are accelerated in common is mathematically identical to the gravitational instability of the interface studied by Lord Rayleigh (see commented references in *Chandrasekhar* [1961]). In *Gratton et al.* [1996], there is a detailed discussion that shows that this concept is appropriate to study the stability of the magnetopause during periods of acceleration produced by fast changes of the solar wind dynamic pressure. We must note that, being subsonic, the dayside magnetosheath plasma moves together with the magnetopause expansion (or compression). The enhancement (or quenching) of the Kelvin-Helmholtz instability by the Rayleigh-Taylor effect over the front side magnetopause, is studied in *Farrugia et al.* [1998b], where piecewise constant profiles are employed to model the magnetopause and its low latitude boundary layer (LLBL).

[16] Since the acceleration episodes last only a finite time, the acceleration of the magnetopause is not uniform, so that the constant parameter g stands for an average value. It is plain that the results of the model are applicable only when the time scale for the growth of the instability is smaller than the period during which the system is accelerated. Several examples of these time scales are reported in the quoted references, but we will return to this point discussing the results in section 3. Pressure balance across the magnetopause is given by the equation $D(p_0 + \mathbf{B_0}\cdot\mathbf{B_0}/8\pi + \rho_0 g y) = 0$, where the operator $D \equiv d/dy$ indicates differentiation with respect to y.

[17] The stability of the equilibrium is studied with the perturbative equations of linearized, ideal (infinite conductivity) magnetohydrodynamics (MHD) [e.g., *Chandrasekhar*, 1961]. The MHD modes are assumed to be of the form $Q_p = Q_1(y)exp[-i\omega t + i\mathbf{k}\cdot\mathbf{x}]$, where Q_p denotes any perturbed quantity, and $Q_1(y)$ is the corresponding amplitude. Here ω is the (generally complex)angular frequency and $\mathbf{k} = (k_x, 0, k_z)$, is the (real) wave number, which lies on the tangent plane.

[18] The linearized continuity equation can be written as

$$\left(\frac{\partial}{\partial t} + \mathbf{v_0}\bullet grad\right)\rho_1 = \left(\frac{d}{dt}\right)_0 \rho_1 = -v_{1y}\frac{d\rho_0}{dy} - \rho_0 div(\mathbf{v_1}).$$

Multiplying by a small time interval, we can set

$$\delta t \times \frac{1}{\rho_0}\left(\frac{d}{dt}\right)_0 \rho_1 = \frac{\delta\rho}{\rho_0} = \left(\frac{\delta\rho}{\rho_0}\right)_{adv} + \left(\frac{\delta\rho}{\rho_0}\right)_{comp},$$

where $(\delta\rho/\rho_0)$ is the relative density perturbation in a time lapse δt, and

$$\left(\frac{\delta\rho}{\rho_0}\right)_{adv} = -\zeta\frac{1}{\rho_0}\frac{d\rho_0}{dy} \quad ; \left(\frac{\delta\rho}{\rho_0}\right)_{comp} = -div\left(\overrightarrow{\xi}\right). \tag{1}$$

We have introduced the perturbative Lagrangian displacements, $\zeta = v_{1y}\delta t$, and $\overrightarrow{\xi} = \mathbf{v_1}\delta t$. The first equation (1) is the relative density change due to density advection, the second is the relative density perturbation due to compressibility. The influence of compressibility on stability is only a small correction when

$$\left(\frac{\delta\rho}{\rho_0}\right)_{comp} \ll \left(\frac{\delta\rho}{\rho_0}\right)_{adv}. \tag{2}$$

From the definition of the sound speed, we have

$$\left(\frac{\delta\rho}{\rho_0}\right)_{comp} = \frac{\delta p}{\rho_0 C_s^2}.$$

The scale length L of the equilibrium density is

$$\frac{1}{\rho_0}\frac{d\rho_0}{dy} \sim \frac{1}{L},$$

and therefore

$$\left(\frac{\delta\rho}{\rho_0}\right)_{adv} \sim \frac{\zeta}{L}.$$

On the other hand, δp can be estimated as

$$\delta p \sim \frac{\zeta}{L}\Delta p_0,$$

where Δp_0 is a characteristic range of variation of the equilibrium pressure, thus

$$\left(\frac{\delta\rho}{\rho_0}\right)_{comp} \sim \frac{\zeta}{L}\frac{\Delta p_0}{\rho_0 C_s^2}, \tag{3}$$

The main branch of the Kelvin-Helmholtz spectrum [*González and Gratton*, 1994] is driven by variations of pressure associated with the kinetic energy available in the unperturbed state, hence

$$\Delta p_0 \sim \rho_0 |\mathbf{v_0}|^2. \tag{4}$$

Therefore inequality 2 holds when the following condition is satisfied

$$\frac{|\mathbf{v_0}|^2}{C_s^2} \ll 1, \tag{5}$$

that is, in subsonic flows compressibility has only a small influence on the main branch of the KH instability.

[19] The case of the secondary, or compressible, branch of the KH instability is excluded from the previous estimate, as it has physical properties different from the main branch. We do not study the compressible branch in this paper. The compressible branch, if excited, has growth rates much smaller than those of the main branch [*González and Gratton*, 1994], although in some cases it may become unstable while the main branch is stable. However, we must not forget that the compressible KH branch and the influence of compressibility on the main branch, become increasingly important as the flow approaches the speed of sound away from the subsolar region, and are essential elements of the stability problem of supersonic flows at the magnetospheric flanks.

[20] Since the magnetosheath flow is subsonic over the dayside magnetopause, the incompressibility approximation ($div(\mathbf{v}) = 0$) is well satisfied. Therefore $Dv_{1y} + i\mathbf{k} \cdot \mathbf{v_1} = 0$, and from $div(\mathbf{B}) = 0$, we have similarly $DB_{1y} + i\mathbf{k} \cdot \mathbf{B_1} = 0$. It is found convenient to work with v_{1y} and B_{1y} as main variables. When $g \neq 0$, ρ_1 is also needed and follows from the continuity equation that, under the incompressible condition, reduces to $v_{1y}D\rho_0 - i\bar{\omega}\rho_1 = 0$. We introduce the following notation

$$\bar{\omega} = \omega - G, \tag{6}$$

with

$$G = \mathbf{k} \cdot \mathbf{v_0}, \tag{7}$$

so that $\bar{\omega}$ stands for the Doppler-shifted frequency. It is also convenient to introduce the function

$$F = \mathbf{k} \cdot \mathbf{B_0}. \tag{8}$$

[21] After some algebraic manipulations the linearized equations for v_{1y}, B_{1y}, and ρ_1 can be conveniently written for numerical computations as

$$\begin{aligned}&\left[D\rho_0(GD - DG) + \rho_0\left(GD^2 - k^2G\right)\right]v_{1y} + ik^2g\rho_1\\ &\quad + (1/4\pi)\left[F\left(k^2 - D^2\right) + D^2F\right]B_{1y} = \omega\left[\rho_0\left(k^2 - D^2\right)\right.\\ &\quad \left. + D\rho_0D\right]v_{1y}, (-F + G)v_{1y} = \omega B_{1y}, -iD\rho_0v_{1y} + G\rho_1 = \omega\rho_1,\end{aligned} \tag{9}$$

where we have set $k = |\mathbf{k}|$. A derivation of the perturbative equations can be found in *Farrugia et al.* [1998b].

[22] The set of equation (9) is of the form of an extended eigenvalue problem $L(X) = \omega M(X)$, where L and M are linear differential operators applied to the vector $X = (v_{1y}, B_{1y}, \rho_1)$, and where the eigenvalue is the complex frequency ω. The operators are then discretized by finite differences, and equation (9) is replaced by a matrix eigenvalue problem that approximates the original one. The boundary conditions require that the perturbative quantities tend to zero far from the gradient region, which is assumed to be in the neighborhood of $y = 0$. Since the boundary conditions are at $y \to \pm\infty$, it is advantageous to carry out the numerical procedure using a stretched coordinate defined as

$$\eta \equiv \begin{cases} -\ln(1 - y) & y < 0, \\ \ln(1 + y) & y > 0. \end{cases}$$

After L and M are written in terms of η, finite differences are applied. This method allows us to have a sufficient number of grid points in the interval where the gradients are concentrated, and to reach large $|y|$ values with a moderate range of $|\eta|$ values (in practice, 3–4).

[23] Here we assume that the equilibrium fields are represented by hyperbolic tangent functions, as indicated explicitly further on. On the magnetosheath side, the asymptotic values for $y \to \infty$ of the unperturbed quantities $\mathbf{v_{01}}$, $\mathbf{B_{01}}$, ρ_{01} are indicated by a subscript 1. Similarly in the magnetosphere, when $y \to -\infty$, the asymptotic values $\mathbf{v_{02}}$, $\mathbf{B_{02}}$, ρ_{02} are denoted with a subscript 2. The width of the transition from magnetosheath to magnetosphere is indicated with $\Delta = 2h$ and h will be taken as unit of length in our calculations. For instance, $\tilde{y} = y/h$, represents a nondimensional coordinate normal to the magnetopause, and $\alpha = kh$ denotes the dimensionless wave number. However, for simplicity of notation, we shall keep the same symbol y for the nondimensional y-coordinate.

[24] In KH stability analysis it is customary to employ the asymptotic values on one side of the gradient region as reference for dimensionless variables. However, in our case the values for the fields and density at different positions on the magnetopause are taken from the MHD magnetosheath model cited in the introduction. This model scales physical quantities with solar wind values before the bow shock, i.e., the solar wind speed, U_{sw}, and density, ρ_{sw}. Thus we normalize our variables using the same units, as follows. We denote the dimensionless equilibrium density with $\tilde{\rho}_0 = \rho_0/\rho_{sw}$, and the normalized amplitude of the density perturbation with $\rho(y) = \rho_1/\rho_{sw}$. Similarly, $\tilde{v}_\mathbf{0} = \mathbf{v_0}/U_{sw}$, $v(y) = v_{1y}/U_{sw}$, indicate the normalized equilibrium velocity, and the perturbative y velocity component, respectively. We also introduce $\tilde{G} = hG/U_{sw}$. The magnetic field intensity will be measured in units of $\sqrt{4\pi\rho_{sw}}U_{sw}$, and we thus set $\tilde{\mathbf{B}}_0 = \mathbf{B_0}/\left(\sqrt{4\pi\rho_{sw}}U_{sw}\right)$, and $b(y) = B_{1y}/\left(\sqrt{4\pi\rho_{sw}}U_{sw}\right)$, for equilibrium and perturbative magnetic field, respectively. Finally we introduce an acceleration unit, $q^{-1} = U_{sw}^2/2h$, we set $\tilde{F} = hF/\left(\sqrt{4\pi\rho_{sw}}U_{sw}\right)$, and define a dimensionless eigenvalue $\tilde{\omega} = h\omega/U_{sw}$.

[25] In dimensionless variables equation (9) can be written as

$$\begin{aligned}&\left[-\tilde{\rho}_0\tilde{G}\left(\alpha^2 - D^2\right) - \tilde{\rho}_0\tilde{G}'' - \tilde{\rho}_0'\tilde{G}' + \tilde{\rho}_0'\tilde{G}D\right]v + i\alpha^2qg\rho\\ &\quad + \left[\tilde{F}\left(\alpha^2 - D^2\right) + \tilde{F}''\right]b = \tilde{\omega}\left[-\tilde{\rho}_0\left(\alpha^2 - D^2\right) + \tilde{\rho}_0'D\right]v,\\ &\quad - \tilde{F}v + \tilde{G}b = \tilde{\omega}b, -i\tilde{\rho}_0'v + \tilde{G}\rho = \tilde{\omega}\rho,\end{aligned} \tag{10}$$

where we have set $f_0' = df_0(y)/dy$, $D\tilde{f} = d\tilde{f}/dy$, and y, as mentioned, is in units of h.

[26] Let us introduce now the dimensionless asymptotic values for the magnetosheath side by $f_v = |\mathbf{v_{01}}|/U_{sw}$, $f_b =$

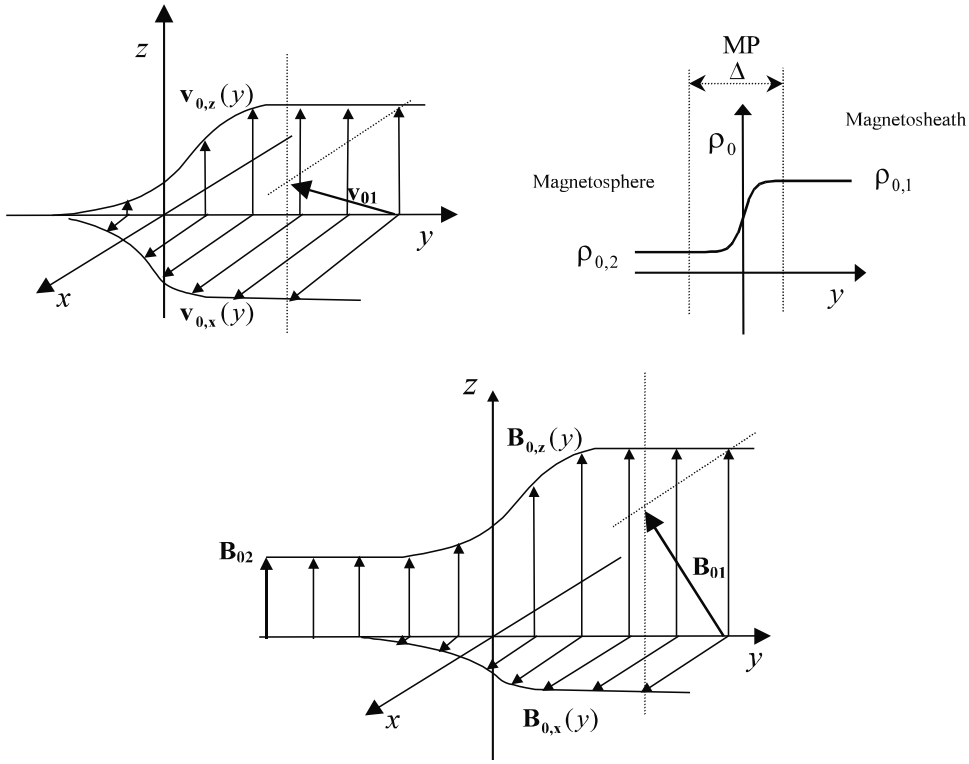

Figure 2. Schematic of the local model for the equilibrium velocity, top left, magnetic field, bottom, and density profile, top right, across the magnetopause, assumed in the stability analysis.

$|\mathbf{B_{01}}|/(\sqrt{4\pi\rho_{sw}}U_{sw})$, $f_d = \rho_{01}/\rho_{sw}$. The corresponding asymptotic values on the magnetosphere side will be defined by the following ratios: $r_v = |\mathbf{v_{02}}|/|\mathbf{v_{01}}|$, $r_b = |\mathbf{B_{02}}|/|\mathbf{B_{01}}|$, $r_d = \rho_{02}/\rho_{01}$. In Figure 2 we show a schematic of the equilibrium fields and density profiles across the magnetopause. We shall take the local z-axis along the geomagnetic field (GMF) $\mathbf{B_{02}}$. The magnetosheath field, in general, will have a shear angle, $\Psi_{B1,B2} \equiv \text{angle}(\mathbf{B_{01}}, \mathbf{B_{02}})$, with respect to the GMF. On the magnetosheath side the velocity field has an asymptotic direction defined by the angle with the GMF, $\Psi_{v1,B2} \equiv \text{angle}(\mathbf{v_{01}}, \mathbf{B_{02}})$. As commented in the introduction, in this study we assume that the velocity does not change direction across the boundary, and tends to zero for $y \to -\infty$.

[27] In order to examine the stability conditions of the magnetopause we consider three positions on the dayside surface, which will be represented by the paraboloid

$$X = 1 - 0.5\left(Y^2 + Z^2\right), \tag{11}$$

where Z points due north, Y toward east and X is along the Sun-Earth direction; X, Y, Z, are in units of the radius of curvature of the magnetopause at the subsolar point. The three cases are on the line corresponding to 14:24 hours, with increasing latitudes, as shown in Figure 3. The figure indicates also the computational grid for the coordinates Y, Z. The three positions are indicated in the first column of Table 1 and correspond to latitudes of 0°, 29.3°, and 41.7°; $f_v, f_b, f_d, r_b, \Psi_{v1,B2}$, and $\Psi_{B1,B2}$, are listed, respectively, in the following columns. The values are taken from the numerical results of the magnetosheath MHD code mentioned before [see, e.g., *Farrugia et al.*, 1998b]. The magnetic shear angle increases from 0 to 21°, while the ratio of inner to outer magnetic field strengths decreases from 1.3 to 0.5 with an increase of latitude of 41.7°. The peculiar trend of variation of the angle $\Psi_{v1,B2}$ is due to the interplay of

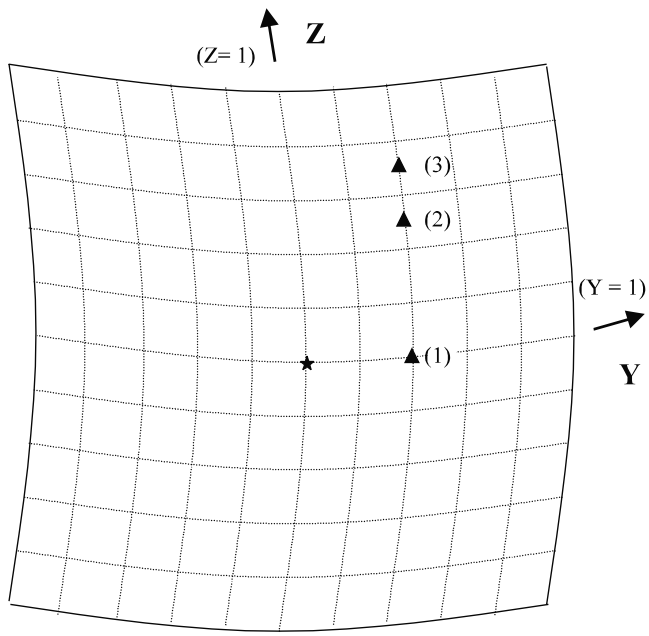

Figure 3. Position of the points of the dayside magnetopause where KH modes are studied. The star indicates the subsolar point. The grid points shown in the figure correspond to the MHD code quoted in the text.

Table 1. Position and Parameters Used in the Stability Analysis

Position	(*X*, *Y*, *Z*)	Latitude	f_v	f_b	f_d	r_b	$\Psi_{v1,\ B2}$	$\Psi_{B1,\ B2}$
1	(0.920,0.4,0.0)	0°	0.2352	1.1994	0.7502	1.2670	90°	0°
2	(0.795,0.4,0.5)	29.3°	0.2658	1.0875	0.7387	0.8935	81°	6°
3	(0.675,0.4,0.7)	41.7°	0.2945	1.0055	0.7259	0.5288	92°	21°

different rates of change in the directions of the geomagnetic field and the velocity field, as we move toward higher latitudes.

[28] In all cases we assume that $r_d = 0.1$, a typical value for the ratio between magnetosheath and magnetospheric density. In equation (10) $qg = 0$ for a static boundary; however, when we compute the effect of an accelerating magnetopause we set $|qg| = 0.0024$. This particular value for the nondimensional acceleration arises from the following assumptions: $|g| = 1\text{km/s}^2$, $\Delta = 2h = 600$ km, $U_{sw} = 500$ km/s. Estimates for g are discussed in [*Sonnerup et al.*, 1987; *Mishin*, 1993; *Gratton et al.*, 1996; *Farrugia et al.*, 1998b]. For Δ we take the average value of the magnetopause thickness derived from a statistical analysis of ISEE 1 and 2 crossings [*Berchem and Russell*, 1982], and U_{sw} is an intermediate value for the solar wind speed.

[29] The following equations define the y dependence of the nondimensional, unperturbed, velocity field, magnetic field, and density distribution:

$$\tilde{v}_{0x} = \sin\Psi_{v1,B2}\cdot m(y)\cdot f_v, \tilde{v}_{0z} = \cos\Psi_{v1,B2}\cdot m(y)\cdot f_v,$$
$$\tilde{b}_{0x} = \sin\Psi_{B1,B2}\cdot m(y)\cdot f_b, \tilde{b}_{0z} = [\cos\Psi_{B1,B2}\cdot m(y) + rb\cdot n(y)]\cdot f_b,$$
$$\tilde{\rho}_0 = [m(\Delta y/\delta) + r_d\cdot n(\Delta y/\delta)]\cdot f_d, \qquad (12)$$

where $m(y) = 0.5\cdot[1 + \tanh(y)]$, and $n(y) = 0.5\cdot[1 - \tanh(y)]$. Here, the x, z components are in a local coordinate system lying in the magnetopause tangent plane, and δ is the scale length of the density profile. According to the analysis of *Eastman et al.* [1996] δ may be different from Δ, when conditions of pristine magnetopause apply, i.e., in the absence of low latitude boundary layer. Our stability analysis will be carried out for two values, $\Delta/\delta = 1$, and 5.

[30] The layout of the model, and the profiles defined by equation (12), show that in this paper we are computing the eigenvalues for a one step transition only. The important influence of the PDL on the instability appears in the asymptotic conditions on the magnetosheath side. But we have not included in the model the field profiles of the PDL. Thus for instance, the increment of inertia as $y > 0$ increases on the magnetosheath side, is not accounted for in the theory. Similarly, on the magnetospheric side, the model does not include the presence of a low latitude boundary layer with its associated inner edge (IEBL), a configuration that requires more than one transition. For certain ranges of wavelength, however, the results of the single transition model can be reinterpreted as indicated in section 5, for applications that need to reckon with the IEBL.

3. Latitude Dependence of the KH Instability

[31] We report now the results of numerical solutions of the equations for the KH modes with the parameters of the three positions of increasing latitude given in Table 1. In all the cases examined in this section we assume $\Delta/\delta = 1$. At each position and any given wavelength, we compute the growth rate varying the orientation of the wave vector **k**, in order to find the mode with the maximum (nondimensional) growth rate $p = \Im(\tilde{\omega}) = \Im(\omega)h/U_{sw}$. Figures 4, Figure 5, and Figure 6 show the maximum growth rate as function of λ/Δ for three values of the acceleration g, at positions 1 to 3, respectively. The lines labeled with $g = 0$ correspond to magnetopauses without acceleration. Two lines corresponding to KH with acceleration $g = 1$ km/s$^2 > 0$ and $g = -1$ km/s$^2 < 0$, are also shown for each position.

[32] Considering first the variations of p for $g = 0$ in Figures 4 to 6, we see that the KH excitation decreases

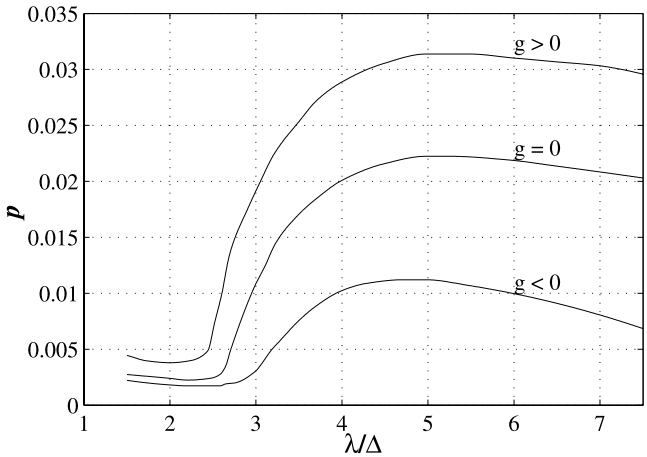

Figure 4. Maximum growth rate p (nondimensional, given in units of $2U_{sw}/\Delta$) as function of λ/Δ for three values of the acceleration g, 1, 0, −1, in km/s^2 at position 1.

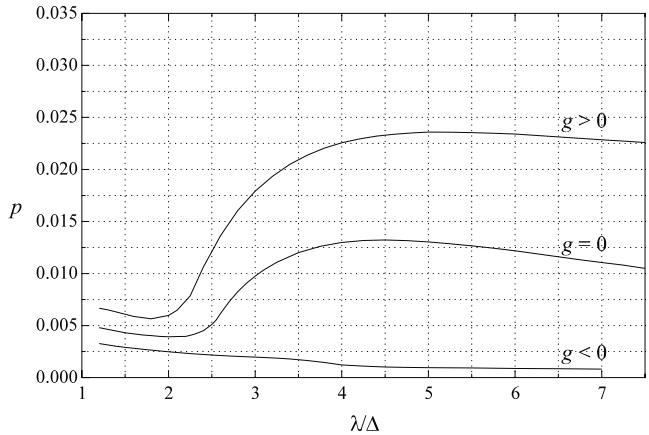

Figure 5. Maximum growth rate p as function of λ/Δ for three values of the acceleration g, with the same format of Figure 4, at position 2.

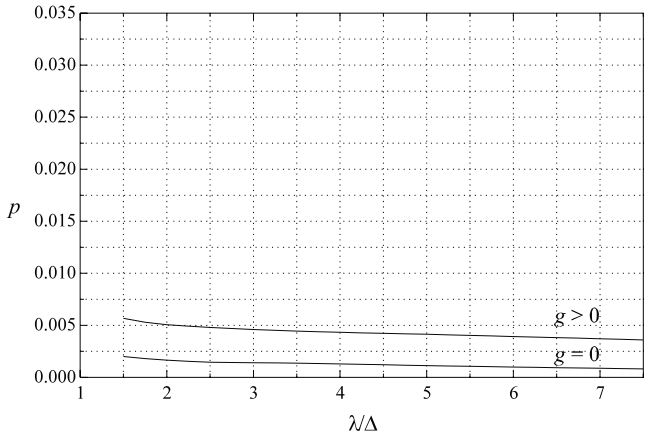

Figure 6. Maximum growth rate p as function of λ/Δ for two values of the acceleration g, 1, 0, with the same units as in Figure 4, at position 3.

substantially with latitude. This is mainly due to the increase of the local magnetic shear. As a consequence, the projection of the velocity on the **k** vector is accompanied by a stabilizing magnetic tension contribution over most of the y range of the perturbation and for all orientations of **k**. In fact, this variation overcomes the effect of the increment of the absolute value of the velocity that increases from positions 1 to 3, while the changes of the velocity angle with respect to the GMF are minor (see Table 1). As a function of λ/Δ the growth rate, which is small for $\lambda/\Delta < 2.5$, increases with λ, and attains a maximum value at $\lambda/\Delta \sim 4.5$ at the positions 1 and 2. It then decreases steadily for longer wavelengths. At position 3 represented by Figure 6, this trend in the growth rate is not evident, but position 3 is only marginally unstable for all λ values. When translated to dimensional values the growth rates for $\lambda \sim 4-8\Delta$ in Figure 4 ($g = 0$) give (with parameter values indicated after Table 1) e-folding times, $\tau_e \sim 50-60$ s. At station 2, the values of p in Figure 5 give $\tau_e \sim 90-120$ s, but the values of p of Figure 6, corresponding to position 3 lead to e-folding times of 14 min. Thus in this case, the flow and magnetic field configuration should remain stationary for very long periods of time in order to produce a significant amplification of KH waves, while the solar wind generally varies on shorter timescales. We conclude that unstable p values in the range 0.002 as in Figure 6 have no practical consequences. The large reduction of the growth rate for $\Psi_{B1,B2} = 21°$ is in qualitative agreement with the growth rate given in [*Miura*, 1995b] for a magnetosheath Alfvénic Mach number, $M_A = 1$, and $\Psi_{B1,B2} = 30°$, whereas we have $M_A = 0.34$ at position 3, as can be computed from Table 1.

[33] We have shown the maximum growth rate: changes with the angle of the wave vector **k** are similar to the well known ones of the tangential discontinuity model, see equation (13) of section 4. The direction of the wave number for the maximum growth rate is nearly normal to the largest magnetic field of both sides, at the three positions studied. These is because the flow is sub-Alfvénic, and the most unstable mode must eliminate the largest magnetic tension, even at the cost of loosing part of the projection of $\mathbf{v}_{01}$ on **k**, the latter being the source of the instability.

[34] The effect of $g \neq 0$ is represented in Figures 4 and 5 with lines labeled $g > 0$ and $g < 0$, while in Figure 6 we show only the line for $g > 0$ because the growth rate for $g < 0$ is negligible.

[35] When applications of these results are considered we must bear in mind that τ_e must be smaller than T_a, a characteristic time of the acceleration episode. Both T_a and g have wide variations, so that any event must be examined on its own. Here we focus attention on large accelerations ($g = 1$ km/s^2) for which *Gratton et al.* [1996] estimated (from a model of the motion of the magnetopause-magnetosheath system) a typical time persistence of g at peak values of the order of 2 minutes. From time to time, observations of large amplitude oscillations of the magnetopause have reported even longer periods.

[36] Sunward accelerations of the magnetopause with $g = 1$ km/s$^2 > 0$ may reduce τ_e by factors of, roughly, 1.4 at station 1 and 1.7 at station 2, enhancing the KH activity. In fact, at the position 3, a sunward acceleration of this magnitude would reduce τ_e to 5–6 min, destabilising this region which was shown to be nearly stable for $g = 0$. One may observe that strong accelerations with definite sign, lasting that long, are not common. On the other hand, we may note that a free oscillation of the magnetopause may last about 7–8 min, typically [*Freeman et al.* [1995], and that *Farrugia et al.* [2000] report a large amplitude oscillation lasting 7.5 min.

[37] At station 1, we can see from Figure 4 that the earthward acceleration reduces the KH instability, but the resulting growth rates are still important. Figure 5 corresponding to position 2, however, shows that $g < 0$ practically stabilize the flow, as the resulting p become similar to those of Figure 6 for $g = 0$.

[38] Figures 7–10, give the spatial shape of several perturbative quantities, i.e., the eigenfunctions corresponding to the KH mode with $\lambda/\Delta = 5$ and the maximum growth rate with respect to all possible orientations of the **k** vector. All eigenfunctions are normalized by setting $v = v_r + iv_i = 1$ at $y = 0$, as can be seen in Figures 7 and 8; this condition automatically sets the scale of the corresponding perturbations b and ρ for the remaining figures. The calculus of eigenvalues is mathematically a homogeneous problem, which allows for an arbitrary normalization of the eigenfunctions. We choose here a simple, yet physically meaningful, convention, setting the amplitude of the velocity perturbation equal unity, midway in the gradient region.

[39] In Figure 7 we show $|v|$ versus η (defined in section 2) in the top panel, with a y scale also given below for easier reference. The bottom panels give similarly, v_r on the left, and v_i on the right. All panels refer to the position 1, and in each one we show results for three g values: $g = 0$ solid line, $g = 1$ km/s^2 dashed line, and $g = -1$ km/s^2 dot-dash trace. Figure 7 shows the typical features of the v_y perturbation for a KH mode, i.e., the gradient region suffers sinusoidal displacements with phase differences (at different positions y) smaller than 90°. We note that the velocity perturbation is stronger on the inner side of the gradient region (magnetosphere). The shape of the velocity eigenfunction is modified when g changes, that is, the asymmetry of $|v|$ increases

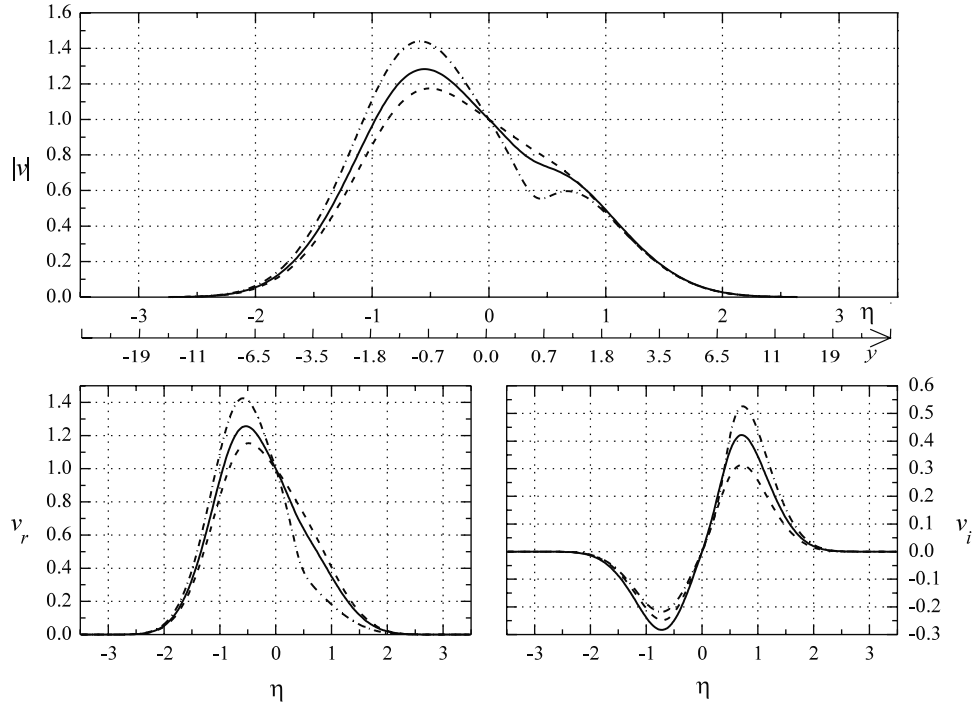

Figure 7. Velocity perturbation, corresponding to the maximum growth rate mode, as function of η for $\lambda/\Delta = 5$ at position 1 for three g values: $g = 0$ solid line, $g = 1$ km/s^2 dashed line, $g = -1$ km/s^2 dot-dash trace. Eigenfuctions are normalized by setting $v = v_r + iv_i = 1$ at $y = 0$. (Top) $|\mathbf{v}|$; (bottom) v_r and v_i.

while the growth rate of the mode decreases, when we compare $g > 0$ with $g < 0$.

[40] Figure 8 shows $|v|$ versus η for two positions, case 2 in the upper panel and case 3 in the lower panel, for the mode of maximum growth rate and $\lambda/\Delta = 5$ as in Figure 7. Here we show results for $g \geq 0$ only, as the growth rates for $g < 0$ are negligible. We note that the velocity perturbation is still larger on the magnetospheric

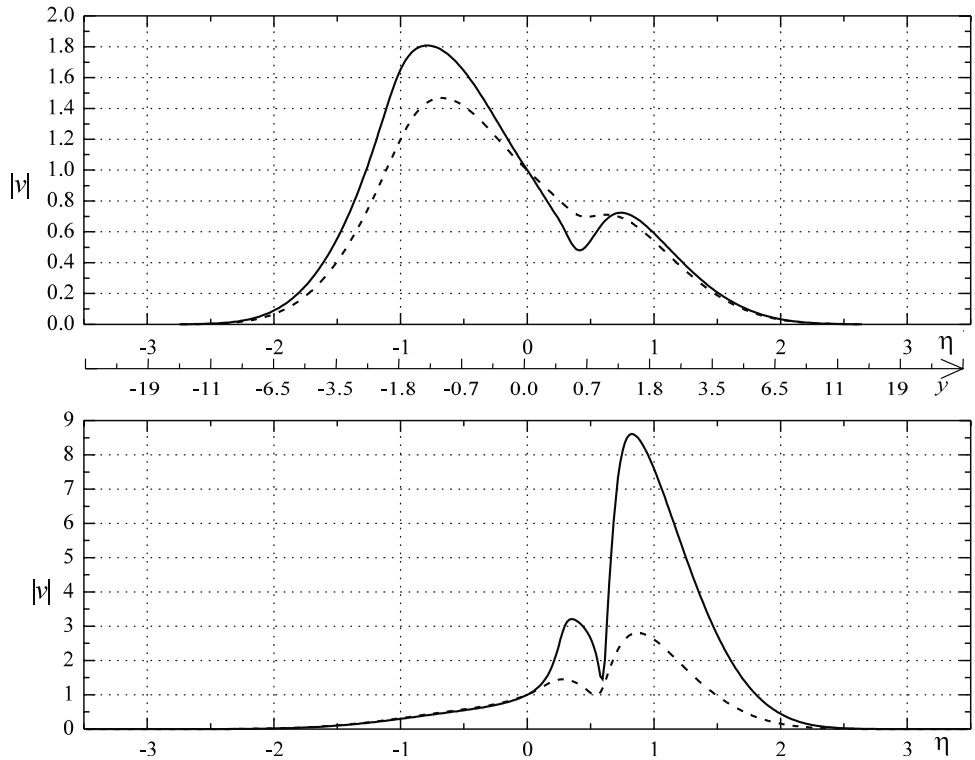

Figure 8. Absolute value of the velocity perturbation, for the maximum growth rate mode, as function of η for $\lambda/\Delta = 5$ at (top) positions 2 and (bottom) 3, for $g = 0$ (solid line) and $g = 1$ km/s^2 (dashed line).

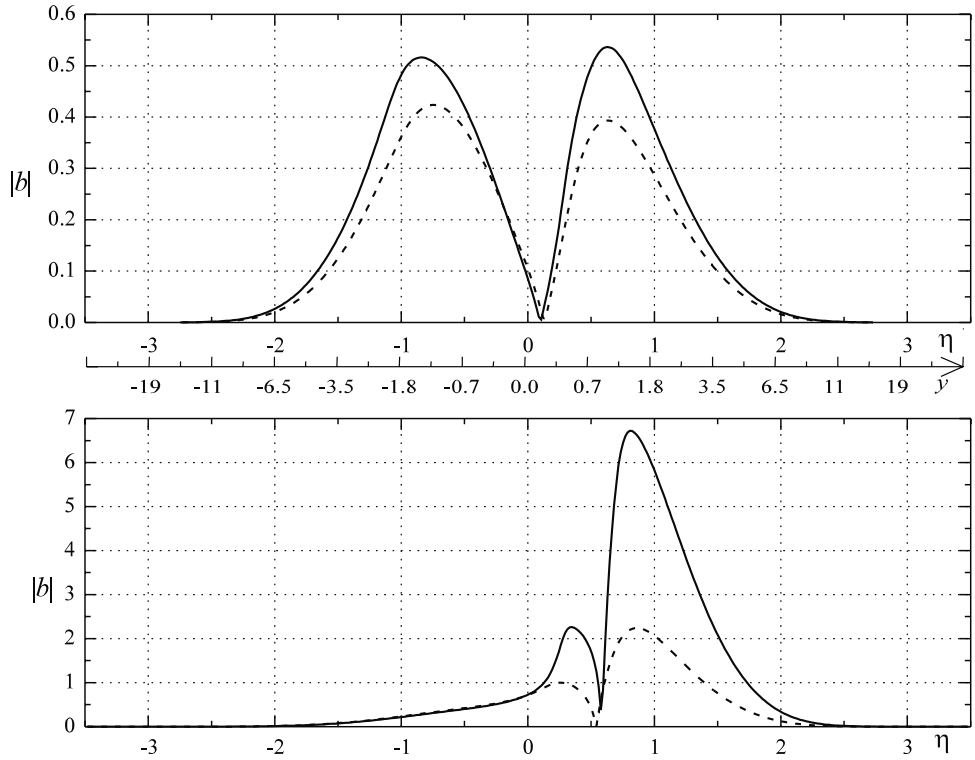

Figure 9. Absolute value of the magnetic field perturbation, for the maximum growth rate mode, as function of η for $\lambda/\Delta = 5$ at positions 2 (top panel) and 3 (bottom panel), for $g = 0$ (solid line) and $g = 1$ km/s^2 (dashed line).

than on the magnetosheath side at position 2, as it was in 1, while the reverse is true at the higher latitude position. We have considered the latter case as practically stable when $g = 0$, but unstable when $g = 1$ km/s^2: we observe that the perturbation occurs mainly on the outside for latitudes where the KH activity is reduced, while it happens for the most part on the inside at lower latitudes, more prone to the KH instability.

[41] The reason for the shift of the perturbation from the magnetospheric to the magnetosheath side of the transition profile, as the latitude increases, is as follow. At the lower latitude, position 1, the wave vector **k** of the mode with maximum growth is normal to the magnetic field on both sides, the shear angle being zero there. For a given amount of kinetic energy of the mode, the amplitude of the velocity perturbation is larger on the magnetospheric side, because of the smaller inertia prevailing there. At the higher latitude, position 3, the GMF has diminished considerably in comparison with the IMF, and even more so the respective magnetic tensions, which are proportional to the square of the fields. Here the vector **k** of the mode of fastest growth becomes normal to the IMF, in order to reduce the largest magnetic tensions. This is an orientation that still gives significant values for the projection of **v** on **k**, on which the instability depends. But now **k** subtends an angle of about 21° with the geomagnetic field, so that the mode suffers the stabilizing effect of the remaining magnetic tensions on the magnetospheric side. Hence, the velocity eigenfunction tends to be localized on the magnetosheath part of the transition, in spite of the larger inertia of that region, to avoid as much as it is possible the residual magnetic tensions. Altogether it results in a considerable decline of the growth rate.

[42] In Figure 9 we show the magnetic field perturbation |**b**| vs. η for the positions 2 (upper panel) and 3 since the modes at position 1 do not entail perturbations in the magnetic field; $|b|$ is represented for the same parameters λ/Δ, p, and g of Figure 8. While the amplitude of the magnetic field perturbation is nearly symmetric with respect to $y = 0$ at position 2, it is localized almost completely on

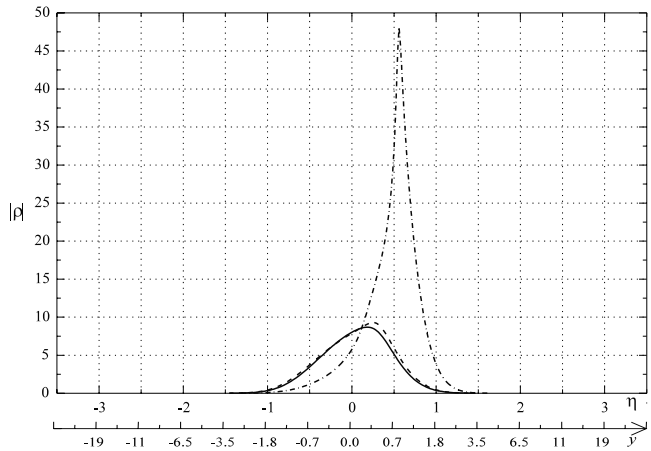

Figure 10. Absolute value of density perturbation, corresponding to the maximum growth rate mode, as function of η for $\lambda/\Delta = 5$ and $g = 1$ km/s^2 at positions 1 (solid line), 2 (dashed line), and 3 (dotted-dashed line).

the magnetosheath side at position 3 instead, as expected from the previous discussion.

[43] In Figure 10 we give an example to illustrate the behaviour of the amplitude of the density perturbation at the three positions examined; we show the $|\rho|$ eigenfunctions for $g = 1$ km/s^2 only, and for the same mode parameters of Figures 8 and 9. Here a solid line corresponds to position 1, and the dashed and dot-dash lines are for positions 2 and 3, respectively. The shift of the density perturbation toward the outside part of the gradient region at position 3 is also apparent.

4. Effect of Two Length Scales on the KH Instability

[44] The current layer at the magnetopause separates the interplanetary magnetic field from the geomagnetic field. In *Eastman et al.* [1996] 235 passes of ISEE 2 (1977–1978) and 125 crossings of AMPTE/CCE (1984–1988) were examined. From these about 10% were identified as pristine cases, defined as those that do not exhibit an adjoining magnetospheric boundary layer or, at most, have a low density plateau. For pristine crossings these authors have reported very sharp density gradients, with scale lengths smaller than those of the current layer region, frequently less than 20%. Thus pristine magnetopauses often exhibit a double scale length feature, although this property is reduced away from noon and tends to disappear at the dawn-dusk meridian.

[45] Motivated by these observations we examine here the influence of a possible difference in the widths of the current layer and the density gradient regions. To find out the consequences of a double-scale assumption on the instability let us reconsider the equatorial position 1, where the current layer, according to our model, is due to the difference of magnetic field intensity (see Table 1). Using the same model for the equilibrium and the perturbative equations given in section 2, we now compute the KH modes with $\Delta/\delta = 5$. Figure 11 summarizes the main results, showing the growth rates as a function of λ/Δ. For each wavelength the corresponding p is the maximum value over all possible $\mathbf{k}$ orientations. There are three lines labeled $g = 0$ corresponding to the KH instability without the assistance of accelerations of the boundary. The line styles distinguish the different assumptions made for the scale lengths. The solid line is for $\Delta/\delta = 5$, and the dashed line corresponds to $\Delta/\delta = 1$, which is shown for comparison. The dotted - dashed line corresponds to the results of a simple tangential discontinuity profile in all equilibrium quantities, computed with the same parameters on both sides of the discontinuity as given in Table 1. Denoting with $\hat{\mathbf{k}}$ a unit vector oriented as $\mathbf{k}$ and using the dimensionless quantities defined in section 2 we can write the dispersion equation for the tangential discontinuity model as

$$\omega h/U_{sw} = \frac{\pi f_v \Delta}{(1+r_d)\lambda}\left[\hat{\mathbf{k}}\cdot\tilde{\mathbf{v}}_{01} \pm \left[\left[\left(\hat{\mathbf{k}}\cdot\tilde{\mathbf{B}}_{01}\right)^2 + \left(\hat{\mathbf{k}}\cdot\tilde{\mathbf{B}}_{02}\right)^2\right](1+r_d)\right.\right.$$
$$\left.\left.\cdot f_b^2 f_v^{-2} f_d^{-1} - r_d\left(\hat{\mathbf{k}}\cdot\tilde{\mathbf{v}}_{01}\right)^2 - \left(1-r_d^2\right) q g f_v^{-2}\pi^{-1}\lambda/\Delta\right]^{1/2}\right] \quad (13)$$

The line for the tangential discontinuity is calculated with this equation. The tangential discontinuity model represents the asymptotic limit of the hyperbolic tangent model as $\lambda/\Delta \to \infty$. We may note that the results of the model with $\Delta/\delta = 5$ differ substantially from those for the case $\Delta/\delta = 1$ at small wavelengths ($\lambda/\Delta \sim 2$–3) where the one-scale model growth rate is strongly reduced while that of the double scale model is still close to its maximum value. Thus for the same λ/Δ ratio in the quoted range, the pristine magnetopause model is KH unstable, while the model with a unique scale length has negligible growth rates. For larger wavelengths $\lambda/\Delta > 5$, however, the two models give qualitatively similar results, with somewhat smaller growth rates in the double scale case. The dotted - dashed line shows how well the tangential discontinuity model, used in many papers as a first estimate for the KH instability, may approximate the model with continuous (hyperbolic tangent) profiles. As expected, the three lines for $g = 0$ converge for long wavelengths, but note that to approximate the growth rate for the continuous one-scale model, with an error not larger than 10%, using the tangential discontinuity KH formula, one must take $\lambda/\Delta > 15$. The three lines with $g = 0$ give growth rates within a 10% difference for $\lambda/\Delta > 20$.

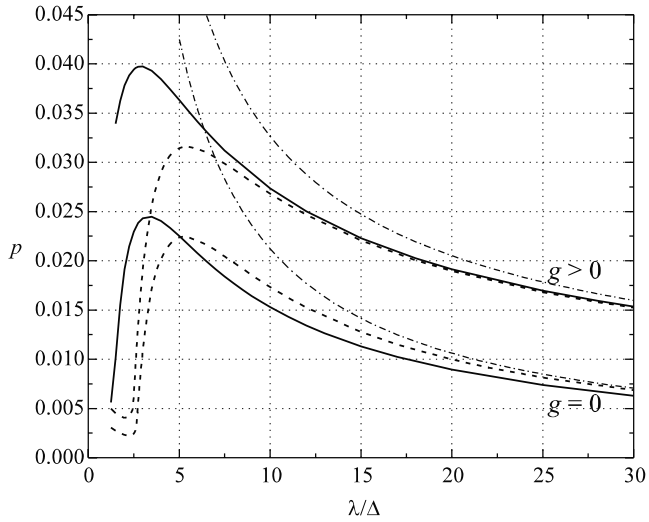

Figure 11. Maximum growth rate as function of λ/Δ, for $g = 1$ km/s^2 and $g = 0$, at position 1 with different assumptions made for the scale length of the equilibrium model (see text). The solid line is for the double scale model, $\Delta/\delta = 5$, the dashed line is for $\Delta/\delta = 1$, and the dotted-dashed line corresponds to the results of a tangential discontinuity model.

[46] The lines labeled $g > 0$ in Figure 11 correspond to sunward accelerated magnetopauses ($g = 1$ km/s^2), the solid line is for the double scale model while the dashed line is for $\delta/\Delta = 1$. Although the maximum growth rate increases, with respect to the $g = 0$ case, as expected (by a factor ~ 1.4–1.6) the behaviour of p versus λ is qualitatively similar to that noted for $g = 0$ at short wavelengths ($\lambda/\Delta < 5$). The ratio of maximum growth rates for $\delta/\Delta = 5$ and $\delta/\Delta = 1$ when $g > 0$, is somewhat larger than the corresponding ratio when $g = 0$ (1.25 versus 1.1), indicating a slight intensification of the instability by the Rayleigh-Taylor effect in the case of the sharper density

gradient model. For long wavelengths ($\lambda/\Delta \sim 7$) the growth rates of the two models approach each other closely, faster than in the $g = 0$ case.

5. Discussions and Conclusions

[47] We have used continuous equilibrium profiles for fields and density to study the properties of the KH instability at the dayside magnetopause, for a configuration with due north IMF. Local parameters for the magnetosheath and magnetospheric sides, at three positions of increasing latitude, have been obtained from the predictions of a numerical MHD model for the magnetosheath. An important element incorporated in the latter calculation is the presence of a plasma depletion layer adjacent to the magnetopause, a feature characteristic of northward pointing IMFs, which is now well confirmed experimentally. In the plasma depletion layer (a) the density decreases while (b) the magnetic field intensity grows, with respect to magnetosheath values. In addition, (c) the velocity field tends to become perpendicular to the IMF, as we move away from the subsolar point. The three effects mentioned all exert an important influence on the development of the KH instability. We have found that the KH excitation decreases substantially with the latitude. This effect is a consequence of the increase of local magnetic shear angle between the magnetosheath and the magnetospheric field, which cancels the effect of increasing velocity. Thus away from the subsolar stagnation point, even when the clock angle $\theta = 0$, which is the most favorable IMF configuration for the KH instability, the activity does not cover the entire dayside magnetopause. We have also noted that the KH perturbation occurs mainly in the magnetosheath part of the velocity gradient region, at latitudes where the KH activity is reduced, while it happens for the most part on the magnetospheric side at lower latitudes, which are more prone to the KH instability. The particular localization of the perturbation eigenfunctions at the high latitude position is due to the decreased intensity of the GMF with respect to the IMF, and to the increment of the magnetic shear angle. In that case, the best chance for the growth of a KH mode relies on a setting in which **k** is perpendicular to the IMF, while the eigenfunction amplitudes are peaked on the magnetosheath side.

[48] In a recent paper we have examined, using only the tangential discontinuity model, the alterations of the main branch of the KH dispersion relation due to compressibility, at the same three magnetopause positions we have considered here. The changes in the growth rate and the unstable range between compressible and incompressible calculations turned out to be insignificant, as expected [*González et al.*, 2002].

[49] We have seen that the stabilization of the high latitude magnetopause is related to the increased magnetic shear angle of this region, and the fact that the orientation of the velocity field tends to become normal to the magnetosheath magnetic field. The latter is a consequence of the plasma depletion layer formation for northward IMFs. As the shear angle increases, the projection of the velocity field on **k** is accompanied with a substantial projection of the magnetic field on **k**, which provides the stabilizing tension. However, the small growth rate at high latitudes, which are marginally stable for a quiescent magnetopause, increases during strong sunward acceleration episodes (as shown in Figures 4 to 6) and the instability may then produce a wavy surface also in these regions. This is a consequence of the Rayleigh-Taylor effect that enhances the Kelvin-Helmholtz instability.

[50] Pristine magnetopauses, i.e., those without boundary layer [*Eastman et al.*, 1996] often exhibit a peculiar double scale length: the density gradient region is thinner than the region where the change of the magnetic field, from magnetosheath to magnetospheric, occur. Stimulated by this fact, we have examined the KH growth rates for a two scale model with $\Delta/\delta = 5$. Significant differences with the model with a unique scale are concentrated mainly at small wavelengths, i.e., $\lambda/\Delta \sim 2-3$, while for longer λ both models give similar growth rates. If we take $\Delta = 600$ km as a typical thickness of the current layer [*Berchem and Russell*, 1982] the maximum growth rates for the "pristine" model occur for $\lambda \sim 1200-1800$ km. These KH perturbations generate surface waves with frequencies, f, of the order of $|v_{01}|/[\lambda(1 + r_d)]$. For the same wavelength range, however, a model with only one scale length gives negligible growth rate for KH modes. The latter case corresponds to magnetopauses with a companion magnetospheric boundary layer.

[51] From this consideration a prediction follows: spacecraft crossings of pristine magnetopauses should observe activity at the ratio $\lambda/\Delta \sim 2-3$ and its corresponding frequency range. But negligible KH activity should be measured at the same λ/Δ ratio, and its associated frequency range, when normal crossings are registered. Thus a correlation of observations during spacecraft crossings with records of magnetic fluctuations of ground magnetometers in the frequency range from 50 to 200 mHz (depending on the local speed $|v_{01}|$) higher than the Pc 5 range ordinarily associated with KH activity, may be attempted to detect a possible enhancement of the power spectrum in the case of pristine magnetopauses, and test this prediction.

[52] The theory with hyperbolic tangent profiles does not take into account specifically the possible presence of a magnetospheric boundary layer. The transition from the magnetosheath to the magnetosphere is assumed to occur in one step only. However, we may note that asymptotically, for $y \rightarrow \pm\infty$, the KH modes decay as $exp(\mp ky)$, so that their penetration length is of the order of $d = \lambda/2\pi$. Therefore we may still apply the hyperbolic tangent model when a second transition (from boundary layer into magnetosphere proper) is present in nature. However, in this case λ must be limited from above, roughly, by $\lambda \leq \Delta_{BL}$, where Δ_{BL} indicates the width of the boundary layer, so that the second transition can be approximately ignored. The width Δ_{BL} may vary widely, but $1/3-1/2\ R_E$ can be taken as indicative values. Moreover, the hyperbolic tangent model can be also applied when $\lambda \gg \Delta_{BL}$, as the magnetopause and the boundary layer can then be lumped together into one transition, ignoring the fine structure with two steps. In the latter case, the width Δ of our theory should be taken as $\sim\Delta_{BL}$.

[53] The model treated here does not include the field profiles of the PDL either. The width of the PDL, variable as it is, can be about 3000 km in average, thus perturbation modes with wavelengths, such that $\lambda > 5\Delta$, lie on a non

uniform density region of the magnetosheath side. Of course, we may expect that modes with very long wavelengths, $\lambda \gg 3000$ km, see again an averaged one step transition, and for them the fine details of the transition from magnetosheath to magnetosphere are erased.

[54] The last two comments (on LLBL and PDL) show that the theory of the MHD stability of the subsolar magnetopause regarding the KH instability is not yet completed. We hope, nevertheless, to have contributed to the understanding of the conditions for the excitation of Kelvin-Helmholtz activity on the dayside.

[55] **Acknowledgments.** We are grateful to N. Erkaev for data of his MHD magnetosheath code used in this study. Work supported in part by Argentinean grants from UBA UBACyT X059, CONICET PIP 2013/01, and by NASA Living with a Star grant NAG 5-10883, and Windgrant NAG 5 - 11803.

[56] Lou-Chuang Lee and Chin S. Lin thank Zuyin Pu and another reviewer for their assistance in evaluating this paper.

References

Belmont, G., and G. Chanteur, Advances in magnetopause Kelvin-Helmholtz instability studies, *Phys. Scr.*, *124*, 1989.

Berchem, J., and C. T. Russell, The thickness of the magnetopause current layer: ISEE 1 and 2 observations, *J. Geophys. Res.*, *87*, 2108, 1982.

Burlaga, L., et al., A magnetic cloud containing prominence material: January 1997, *J. Geophys. Res.*, *103*, 277, 1998.

Chandrasekhar, S., *Hydrodynamic and Hydromagnetic Stability*, Oxford Univ. Press, New York, 1961.

Chen, S.-H., and M. G. Kivelson, Nonsinusoidal waves at the Earths magnetopause, *Geophys. Res. Lett.*, *20*, 2699, 1993.

Chen, S.-H., M. G. Kivelson, J. T. Golsling, R. J. Walker, and A. J. Lazarus, Anomalous aspects of magnetosheath flow and of the shape and oscillations of the magnetopause during an interval of strongly northward magnetic field, *J. Geophys. Res.*, *98*, 5727, 1993.

Dungey, J. W., Electrodynamics of the outer atmospheres, *Sci. Rep. 69*, Penn. State Univ., Ionosphere Res. Lab., State College, Penn., 1954.

Eastman, T. E., S. A. Fuselier, and J. T. Gosling, Magnetopause crossing without a boundary layer, *J. Geophys. Res.*, *101*, 49, 1996.

Erkaev, N. V., Results of the investigation of MHD flow around the magnetosphere, *Geomagn. Aeron.*, *28*, 455, 1988.

Farrugia, C. J., F. T. Gratton, L. Bender, J. M. Quinn, R. B. Torbert, N. V. Erkaev, and H. K. Biernat, Recent work on the Kelvin-Helmholtz instability at the dayside magnetopause and boundary layer, in *Polar Cap Boundary Phenomena*, edited by J. Moen et al., pp. 1, *Kluwer Acad.*, Norwell Mass., 1998a.

Farrugia, C. J., F. T. Gratton, L. Bender, H. K. Biernat, N. V. Erkaev, J. M. Quinn, R. B. Torbert, and V. Dennisenko, Charts of joint Kelvin-Helmholtz and Rayleigh-Taylor instabilities at the dayside magnetopause for strongly northward interplanetary magnetic field, *J. Geophys. Res.*, *103*, 6703, 1998b.

Farrugia, C. J., et al., Coordinated Wind, Interball/tail, and ground observations of Kelvin-Helmholtz waves at the near-tail, equatorial magnetopause at dusk: January 11, 1997, *J. Geophys. Res*, *105*, 7639, 2000.

Farrugia, C. J., F. T. Gratton, and R. Torbert, Viscous-type processes in the solar wind - magnetosphere interaction, *Space Science Review*, *95*, 443, 2001.

Freeman, M. P., N. C. Freeman, and C. J. Farrugia, Magnetopause dynamics in a Newton-Busemann approach, *Ann. Geophys.*, *13*, 905, 1995.

González, A. G., and J. Gratton, The role of a density jump in the Kelvin-Helmholtz instability of a compressible plasma, *J. Plasma Phys.*, *52*, 223, 1994.

González, A. G., J. Gratton, F. T. Gratton, and C. J. Farrugia, Compressible Kelvin-Helmholtz instability at the terrestrial magnetopause, *Brazilian J. Phys.*, *32*, 945, 2002.

Gratton, F. T., C. J. Farrugia, and S. W. Cowley, Is the magnetopause Rayleigh-Taylor unstable sometimes?, *J. Geophys. Res*, *101*, 4929, 1996.

Kennel, C. F., *Convection and Substorms*, Oxford Univ, Press, New York, 1995.

Kivelson, M. G., and S.-H. Chen, The magnetopause: surface waves and instabilities and their possible dynamical consequences, in *Physics of the Magnetopause*, *Geophys. Monogr. Ser.*, vol. 90, edited by P. Song, B. U. Ö. Sonnerup and M. F. Thomsen, pp. 257, AGU, Washington D. C., 1995.

Kivelson, M. G., and Z.-Y. Pu, The Kelvin Helmholtz instability on the magnetopause, *Planet. Space. Sci.*, *32*, 1335, 1984.

Kivelson, M. G., and D. J. Southwood, Coupling of global magnetospheric MHD eigenmodes to field line resonances, *J. Geophys. Res.*, *91*, 4345, 1986.

Mishin, V. V., Accelerated motions of the magnetopause as a trigger of the Kelvin-Helmholtz instability, *J. Geophys. Res.*, *98*, 21,365, 1993.

Miura, A., Anomalous transport by magnetohydrodynamic Kelvin-Helmholtz instabilities in the solar wind-magneotosphere interaction, *J. Geophys. Res.*, *89*, 801, 1984.

Miura, A., Kelvin-Helmholtz instability at the magnetopause: computer simulations, in *Physics of the Magnetopause*, *Geophys. Monogr. Ser.*, vol. 90, edited by P. Song, B. U. Ö. Sonnerup, and M. F. Thomsen, pp. 285, AGU, Washington D. C., 1995a.

Miura, A., Dependence of the magnetopause Kelvin-Helmholtz instability on the orientation of the magnetosheath magnetic field, *Geophys. Res. Lett.*, *22*, 2993, 1995b.

Miura, A., and P. L. Pritchett, Non local Stability analysis of the MHD Kelvin-Helmholtz instability in a compressible plasma, *J. Geophys. Res.*, *87*, 7431, 1982.

Ogilvie, K. W., and R. J. Fitzenreiter, The Kelvin-Helmholtz instability at the magnetopause and inner boundary layer surface, *J. Geophys. Res.*, *94*, 15,113, 1989.

Phan, T.-D., G. Paschmann, W. Baumjohann, N. Sckopke, and H. Lühr, The magnetosheath region adjacent to the dayside magnetopause: AMPTE/IRM observations, *J. Geophys. Res.*, *99*, 121, 1994.

Seon, J., L. A. Frank, A. J. Lazarus, and R. P. Lepping, Surface waves on tailward flanks of the Earth's magnetopuse, *J. Geophys. Res.*, *100*, 11,907, 1995.

Song, P., R. C. Elphic, and C. T. Russell, ISEE 1 and 2 observations of the oscillating magnetopause, *Geophys. Res. Lett.*, *15*, 744, 1988.

Sonnerup, B. U. Ö., The reconnecting magnetopause, in *Magnetospheric Physics*, edited by B. M. McCormac, p. 23, D. Reidel, Norwell, Mass., 1974.

Sonnerup, B. U. Ö., I. Papamastorakis, G. Paschmann, and H. Lühr, Magnetopause propeties from AMPTE/IRM observations of the convection electric field: Method development, *J. Geophys. Res*, *92*, 12,137, 1987.

J. E. Contin, Universidad Tecnológica Nacional, Facultad Regional Haedo, Paris 532, Haedo, Pcia. Buenos Aires 1707, Argentina. (jecontin@hotmail.com)

F. T. Gratton, Instituto de Física del Plasma, Depto. de Física, Facultad de Ciencias Exactas y Naturales, Cdad. Universitaria, Pabellón 1 Buenos Aires 1428, Argentina. (faustogratton@infip.org)

C. J. Farrugia, Space Science Center, University of New Hampshire, College Rd., Morse Hall, Durham, NH 03824, USA. (ferrugia@unhedi2.sr.unh.edu)